PNAS
www.pnas.org

Supplementary Information for

Diverse conjugative elements silence natural transformation in *Legionella* species

Isabelle Durieux[1,#], Christophe Ginevra[2,3,#], Laetitia Attaiech[1], Kevin Picq[1], Pierre-Alexandre Juan[1], Sophie Jarraud[2,3], Xavier Charpentier[1]*

[1] CIRI, Centre International de Recherche en Infectiologie, Team "Horizontal gene transfer in bacterial pathogens", Inserm, U1111, Université Claude Bernard Lyon 1, CNRS, UMR5308, École Normale Supérieure de Lyon, Univ Lyon, 69100, Villeurbanne, France
[2] CIRI, Centre International de Recherche en Infectiologie, Team "Pathogenesis of *Legionella*", Inserm, U1111, Université Claude Bernard Lyon 1, CNRS, UMR5308, École Normale Supérieure de Lyon, Univ Lyon, 69008, Villeurbanne, France
[3] Centre National de Référence des Légionelles, Centre de Biologie et de Pathologie Est, 59 Boulevard Pinel, 69677 Bron Cedex, France

# These authors contributed equally

* Corresponding author: xavier.charpentier@univ-lyon1.fr

This PDF file includes:

Supplementary Results and discussion

Conjugative transfer of pLPL inhibits natural transformation of its new bacterial hosts

We here tested the hypothesis that acquisition of pLPL by conjugation inhibits natural transformation of the plasmid's new host. We thus needed to select the conjugative transfer of pLPL to new hosts. As donor strain, we used isolate 3009 carrying pLPL^{3009KF}. This plasmid results from the insertion of the selectable/counter-selectable "kan-mazF" cassette in a pseudogene of the pLPL of isolate 3009 (pLPL^{3009}). The kan-mazF cassette consists of the *npt*II gene (conferring resistance to kanamycin), the *lacI*q gene and of the *mazF* gene under the *tac* promoter (1). Addition of IPTG induces expression of the MazF toxin and the death of the cells. This construct was initially designed to allow the isolation of 3009 that spontaneously lost pLPL^{3009KF}. Growth curves of the strains in 96-well plate revealed that pLPL^{3009KF} affected the growth rate (Fig. S4A) and its loss restored normal growth to isolate 3009. Even in the absence of IPTG, we know the *tac* promoter to be leaky. Hence, a low expression level of the MazF toxin may be responsible for the reduced growth rate of strain pLPL^{3009KF}.

In spite of the impact of pLPL^{3009KF} on growth, the selectable marker (kanR) allowed for isolation of transconjugants. As recipient, we selected the Paris strain and two other transformable isolates of the ST1 cluster. Spontaneous streptomycin-resistant mutants of each of the three strains were first isolated. Strain 3009 pLPL^{3009KF} was mated with the streptomycin-resistant isolates of the ST1 strains and we selected transconjugants resistant to kanamycin and streptomycin. Consistent with the cost of pLPL^{3009KF} observed in 3009, growth curve experiments in a 96-well plate showed that the transconjugants have a reduced growth rate (Fig. S4B). In 13-mL culture tubes, we confirmed that the cultures of the transconjugants could reach an optical density of ~5 rather than the OD of ~6, typically observed for the Paris strains and isolates of the ST1 cluster. Although growing more slowly, the culture of the transconjugant Paris pLPL^{3009KF} nonetheless goes through the transition phase at which expression of the DNA uptake system (and natural transformation) occurs (OD 2-3 in culture tube or Abs 0.4-0.7 in 96-well cultures, grayed area). However, the transconjugant Paris pLPL^{3009KF} never expressed *comEA* during growth (Fig. S4C) and none of the transconjugants of the ST1 strains could undergo natural transformation (Fig. S4D). In contrast, and despite a similarly affected growth, a transconjugant of the Paris strain carrying pLPL^{3009KF} deleted of *rocRp* could express *comEA* and undergoes natural transformation (Fig. S4C and S4E). Altogether, the data demonstrate that pLPL can transfer by conjugation to new hosts and express RocRp to silence expression of the DNA uptake system thereby inhibiting natural transformation.

Supplementary Material and methods

DNA manipulation, plasmid construction

All PCR for assembling transforming DNA were obtained by proof-reading polymerase (PrimeStar Max, Takara). Genomic DNA from Legionella was isolated using the Wizard Genomic DNA Purification Kit or the Maxwell DNA extraction kit (Promega). Plasmids from *L. pneumophila* were isolated from 25 mL of culture using the alkaline lysis method, followed by extraction with phenol:chloroform:isoamyl alcohol (25:24:1) followed by ethanol precipitation. The pellet was treated with RNAse A, ethanol-precipitated and resuspended in 50 µL of Tris-HCl 10 mM, pH 8.

Construction of plasmid pX3-rocRp: the *rocR-like* gene was obtained by PCR on *L. pneumophila* Lens DNA using primers KP1 and KP2. The PCR product was purified by gel electrophoresis and silica-based gel extraction. The pX3 plasmid (an RSF1010 derivative) (2) and the PCR product were then digested by XmaI and NotI and ligated overnight at 16°C. The ligation reaction was used to transform chemically-competent *E.coli* (DH5α). Transformants were selected on LB (Lysogeny Broth) Agar supplemented with 25 µg/mL chloramphenicol. One colony was used to start a culture in liquid media LB supplemented with 25 µg/mL chloramphenicol and then a plasmid extraction was performed. The obtained plasmid pX3-rocR-like was validated by restriction profiling and Sanger sequencing. *L. pneumophila* Paris WT, *rocC*$_{TAA}$

and Δ*rocR* were then transformed by electroporation (2,4 kV, 100 Ω, 25 mF). Transformants were selected on CYE supplemented with 5 µg/mL chloramphenicol.

Mutant strain construction

Full sequence of all genetic constructs are available upon request.

(A) Construction of derivatives of HL-0640-3009.

Strain 3009 pLPL^{3009KF} was obtained by introducing the kan-mazF cassette (1) at position 9074 (between CDS55 and CDS56) of the pLPL plasmid carried by HL-0640-3009. Isolate HL-0640-3009 was naturally transformed with a PCR product consisting of the kan-mazF cassette flanked by 2 kb of sequences corresponding to the insertion site. Three PCR fragments were generated independently, a 2 kb PCR fragment upstream of the targeted insertion site (primers mazF-pLPL_P1F and mazF-pLPL_P2F), a PCR product of the kan-mazF cassette (primers MazFk7-F and MazFk7-R) and a PCR product of a 2kb fragment downstream of the targeted insertion site (primers mazF-pLPL_P1F and mazF-pLPL_P2F). The PCR products were purified, mixed and the assembled PCR product was amplified with primers mazF-pLPL_P1F and mazF-pLPL_P4F. HL-0640-3009 was then naturally transformed with this DNA construct. Due to the low transformability of the isolate (transformation frequency ~1E-8), only a handful of transformants were obtained. The transformants are resistant to kanamycin and sensitive to IPTG (because it induces expression of the MazF toxin). Correct insertion was validated by PCR. Strain 3009ΔpLPL was isolated by plating culture of strain 3009 pLPL^{3009KF} on CYE plates containing IPTG. Clones resistant to IPTG and sensitive to kanamycin were found to lack the entire pLPL. Plasmid extraction and PCR analysis confirmed the absence of pLPL. Strain 3009Δ*rocRp* was obtained in two steps. First, the kan-mazF cassette was inserted in the *rocRp* gene by following the same method used for inserting the cassette in between CDS55 and 56 (see above). As described above, a PCR product was assembled with a 2 kb fragment upstream of *rocRp* (PCR with primers DeltaRocRlike_P1 and DeltaRocRlike_P2), a PCR product of the kan-mazF cassette (primers MazFk7-F and MazFk7-R) and a PCR product of a 2kb fragment downstream of *rocRp* (DeltaRocRlike_P3 and DeltaRocRlike_P4). Isolate HL 0640 3009 was naturally transformed with the PCR product and transformants were selected on kanamycin. Correct insertion of the kan-mazF cassette was verified by PCR. Second, the strain was naturally transformed with a PCR product creating a internal deletion of *rocRp*. The PCR product consists of the assembly of two PCR products corresponding to the upstream (primers DeltaRocRlike_P2d and DeltaRocRlike_P3d) and downstream sequence of *rocRp* (Primers DeltaRocRlike_P1 and DeltaRocRlike_P4). Transformants were selected on IPTG and were checked for sensitivity to kanamycin. Plasmid extraction and PCR analysis confirmed that pLPL was still present in the isolate and that *rocRp* was effectively deleted.

(B) Conjugative transfer of pLPL^{3009KF} to JR32, Paris and other clinical isolates.

Streptomycin-resistant mutant of isolates of LG-0712-2011, Paris and HL-0638-5028 were obtained by plating 1 mL of culture on CYE plated containing streptomycin and isolating spontaneous resistant mutants. JR32 is readily resistant to streptomycin. The streptomycin resistant recipients were inoculated in 3 mL of AYE medium together with the streptomycin-sensitive strain 3009 pLPL^{3009KF} at OD=0.1 in 13-mL tubes. The cultures were grown for 48H at 30°C in a shaking incubator and 100 µL were then plated on CYE containing kanamycin and streptomycin. Cultures of recipients or donor alone did not give rise to colonies. Presence of the pLPL^{3009KF} plasmid in the transconjugants was confirmed by plasmid extraction and PCR analysis. The donor isolate, HL-0604-3009 shows an atypical growth curve with a stationary phase (OD=3.9-4.2) lower than most *L. pneumophila* isolates (OD=5.5-6.0), including the recipients. This phenotype was used to verify that kanamycin and streptomycin resistant mutants corresponded to transconjugants rather than spontaneous streptomycin resistant mutants of the donor.

(C) Construction of Paris strain carrying *rocRp* on plasmid pLPP.

The *rocRp* gene was introduced in the pseudogene *plpp0110* of pLPP by natural transformation of the Paris strain. A PCR product was assembled using 2 kb of sequence upstream of *plpp0110* (primers plpp0110_P1 and plpp0110_P2g), the *rocRp* gene (primers KP1 and KP2), the gentamicin resistance gene (primers gnt-F and gnt-R) and 2k of sequence downstream of *plpp0110* (primers plpp0110_P3g and plpp0110_P4). The assembled PCR product was added to a liquid culture of the Paris strain and incubated 24h at 30°C for natural transformation to occur. Transformants were selected on CYE plates with gentamicin. Presence of the *rocRp* gene in pLPP was confirmed by PCR.

(D) Construction of strain Paris_H1.

Paris_H1 carries the *sfgfp* gene, encoding superfolder GFP, under the strong promoter J23119 (iGEM part Bba_J23119) inserted in the pseudogene *lpp0858a*. The strain was obtained by natural transformation of a PCR product assembled from four PCR products: a PCR consisting of 2 kb upstream of the targeted insertion site (primers lpp0858_P1 and lpp0858_P2), a PCR product of the *sfgfp* gene under the stong promoter J23119 (primers J23119 and termR), a PCR product of the gentamicin resistance gene (primers gnt-F and Cassette_Gm_Rv) and a PCR product of 2 kb of sequence downstream of the targeted insertion site (primers lpp0858_P7 and lpp0858_P8).

Quantitative transformation assays

The tested strains were inoculated at OD = 0.1-0.2 in 3 mL of AYE in 13 mL tubes. One microgram of transforming DNA was added and the cultures were incubated at 30°C with shaking for 24H. A PCR product of encompassing the *rpsL* gene from the Paris_S strain was used for streptomycin-sensitive strains. Alternatively, transformation was tested with a non-replicative circular DNA carrying the kanamycin resistance gene inserted in the non-essential *ihfB* gene (pGEM-ihfB::kan) (2). For strains resistant to both kanamycin and streptomycin (*i.e.*, Paris_S pLPL^{3009KF}) transformation was tested with genomic DNA of strain Paris_H1 which carries the gentamicin resistance gene inserted in the pseudogene *lpp0858a*. Transformation with genomic DNA typically yields 10- to 100-fold lower transformation frequencies than PCR product or plasmid. Transformation frequencies were obtained by calculating the ratio of transformants CFU over total CFU counts, determined by plating serial dilution on selective and non-selective CYE plates. All transformation assays were performed at least three times independently, several days or weeks apart.

Transformation assay of clinical isolates and GWAS

From a culture on CYE plate, clinical isolates (see Table S1) were grow in 100 µL of AYE in 96-well plates sealed with oxygen-permeable membrane (Sigma-Aldrich) at 30°C with shaking at 200 rpm (Infors HT) for 24H. Cultures were homogenized by pipetting and 2 µL were transferred to 100 µL of AYE containing 2 µg/mL of PCR product (primers rpsL_Fw and rpsL_Rv) of the *rpsL* gene region of the Paris_S strain. The plates were sealed with an oxygen-permeable membrane and incubated at 30°C in a shaking Thermomixer (Eppendorf) at 600 rpm. Control experiments were run in parallel, in the same conditions but without added DNA. After 48h, 10 µL of cultures were then spotted on CYE plates containing streptomycin and incubated at 37°C for three days. Each 96-well plate contains a transformable control strain (Paris) and a control streptomycin-resistant strain (JR32). Transformation was scored as a function of the approximate number of colonies that developed in the spot (no colony, score 0; 1 to 9 colonies, score 1; 10-50 colonies, score 2; so many colonies that the spot appears smooth, score 3). Transformation scores were determined four times independently. For each experiment, a score was retained only if it was superior to the score determined in the no DNA condition. A median score was then calculated for the *n* number of determinations that met this criteria. Phylogenetic relationships were determined using cgMLST generated with chewBBACA (3) and vizualised using GrapeTree (4). GWAS were carried out using DBGWAS 0.5.2 (5) on a binary matrix of non-transformable (NT, score 0-0.5) and transformable (T, score 1-3) phenotypes.

Gene expression analysis by northern-blot

Total RNA from bacterial cultures was extracted according to a previously described procedure (6). Briefly, bacterial cultures (1 mL) were mixed to an equal volume of ice-cold methanol, pelleted and lysed in 50 µl of RNAsnap buffer (18 mM EDTA, 0.025% SDS, 95% formamide). RNA was then extracted using a tri-reagent solution (acid guanidinium thiocyanate–phenol–chloroform) and isopropanol-precipitated. One to two micrograms of total RNA in denaturing buffer were loaded per lane of a denaturing Tris/Borate/EDTA (TBE)–urea 8% acrylamide gel. Ethidium-bromide staining of ribosomal RNA was used to check for equal loading of the lanes. RNA was transferred to a nylon membrane and cross-linked by UV irradiation. Membranes were hybridized at 42 °C with 5 nM of a 5′-biotinylated oligonucleotide probe (Table S4) in ULTRAhyb Ultrasensitive Hybridization Buffer (Ambion) and then washed according to the manufacturer's instructions. Membranes were developed using HRP-conjugated streptavidin and enhanced luminol substrate (Pierce). Luminescence signals were acquired using an imaging workstation equipped with a charge-coupled device camera (Vilber-Lourmat).

Purification and relative quantification of RocC-bound RNAs

The RNA-Immunoprecipitation (RIP) procedure was done as described previously (7). Briefly, bacterial cultures at the indicated optical densities were fixed with 1% formaldehyde for 30 min. Pelleted bacterial cells were resuspended in lysis buffer (50 mM HEPES-KOH pH7.5, 150mM NaCl, 1 mM EDTA, 1% Triton X-100, 0.1% Na-deoxycholate) and sonicated at 4°C. Lysates were incubated with Dyna-beads Protein A magnetic beads (Invitrogen) coated with rabbit-raised affinity-purified antibodies directed against RocC. Following washing steps, RNA were eluted from the magnetic beads by extraction with a tri-reagent solution (acid guanidinium thiocyanate-phenol-chloroform) and isopropanol-precipitated. RNA were reverse-transcribed (RevertAid, Thermo) in a single reaction with a mix of two primers specific for RocRp and RocR (primers RT19-rocRlike and RT20-rocR). Both primers carry a 5' extension which was then used for the simultaneous PCR amplification of RocR and RocRp with primers RRl17F and RRl20R. The resulting PCR product, a mix of RocR (86 bp) and RocRp (85 bp), were purified and digested with NruI, which cleaves only RocRp, giving two fragments of 42 and 43 bp. The restriction digests were quantified by capillary electrophoresis (TapeStation, Agilent).

5′/3′ RACE of RocR and RocRp

5′/3′ RACE was performed essentially as previously described (8). Briefly, total RNA (5 µg) was treated with RppH (New England Biolabs) for 1 h at 37°C. After purification using the DirectZol kit (ZymoResearch), RNA was circularized with T4 RNA ligase overnight at 16°C. The ligase was inactivated by a 15 min-incubation at 70°C and RNA was purified using the DirectZol kit. RocR and RocRp were then reverse-transcribed with a specific primer (LA124) using the RevertAid H Minus kit (ThermoFischer). The PrimeSTAR Max (TaKaRa) was used to PCR-amplify either RocR (primers LA124 and LA125) and/or RocRp (primers LA124 and LA126). The PCR products were cloned using the CloneJET system (ThermoFischer) and sequenced.

Genomes sequencing, assembly and analysis

Environmental isolates of *L. geestiana* and *L. israelensis* were sequenced using both Illumina and Oxford Nanopore technologies. For Illumina sequencing, whole genomes were sequenced in paired-end 2x300 bp on a Miseq sequencer using Nextera XT kit according to manufacturer's instructions. For Nanopore sequencing, whole genomes were sequenced using the Rapid barcoding kit on a MinION sequencer according to manufacturer's instructions (Oxford Nanopore). Illumina reads were trimmed for low quality nucleotides and adapters removing using trimmomatic 0.36 (9). Nanopore reads were base-called and demultiplexed using guppy (Oxford Nanopore). Illumina and Nanopore reads were then used for short reads/long reads hybrid assembly using Unicycler v0.4.6 (10). Similarly, the genomes of *L. israelensis* ATCC43119 and *L. geestiana* ATCC49504 were assembled from raw Illumina and Pacbio sequencing data downloaded from NCBI SRA database. All genomes were annotated using prokka 1.13 (11). Presence of *rocR* and *rocRp* sequences in *Legionella* genus

genomes were investigated using local blastn on all the 835 *Legionella*/*Fluoribacter*/*Tatlockia* genome assemblies (697 *Lp*, 138 non-*Lp*) available from the NCBI assembly database on March 6th, 2019. Detection of conjugative elements was performed using MacSyFinder (12) and the ConjScan module (13).

Tables S1 to S5

Table S1. Transformation scores of strains and clinical isolates for GWAS.

Natural transformability was tested in 96 well plates. Transforming DNA (a 4kb PCR product encompassing the *rspL* gene of the streptomycin-resistant mutant Paris_S) is added to 100 µl of AYE inoculated with the isolate. The culture was incubated 48H at 30°C with orbital shaking. A 10 µl sample was then spotted on a CYE plate containing streptomycin (50 µg/mL) and incubated for 3 days at 37°C. Transformation was scored as a function of the approximate number of colonies that developed in the spot (score 0 = no colony; score 1 = 1 to 9 colonies; score 2 = more than 10 colonies but still distinguishable; score 3 = so many colonies that the spot appears smooth). Transformation scores was determined four times independently. A control without DNA is conducted in parallel. For each experiment, a score is retained only if it is superior to the score determined in the no DNA conditions. The median score is reported for the n number of determinations that met this criteria. Isolates are considered transformable (T) if the median score is higher than 0.5, otherwise they are considered non-transformable (NT). Sequence-types (ST), presence of a pLPL plasmid and *rocRp*, and the average transformation frequencies determined using the *ihfB*::kan marker (TF (*ihfB*::kan)) are also reported.

Isolate	ST	pLPL	rocRp	MEDIAN SCORE	T/NT	n=	TF (*ihfB*::kan)
Paris	1			2	T	4	1.2E-05
HL 0618 5018	23			2	T	4	
HL 0620 4017	40			0	NT	4	
HL 0622 5007	23			1	T	3	
HL 0622 5017	40			0	NT	4	
HL 0623 2008	23			1.5	T	4	
HL 0624 5009	23			2	T	4	1.3E-07
HL 0626 3008	664			1	T	4	2.2E-07
HL 0626 3031	317			2	T	4	
HL 0627 4016	700			1	T	3	
HL 0629 2024	44			1	T	4	
HL 0629 4018	23			0	NT	3	5.8E-09
HL 0631 1018	146			0.5	NT	4	3.5E-08
HL 0631 2017	1			2.5	T	4	
HL 0631 2018	700			0.5	NT	4	
HL 0631 3013	455			0	NT	4	5.6E-08
HL 0633 3016	26			0	NT	3	
HL 0633 5004	23	+	+	0	NT	3	
HL 0634 5015	441			2.5	T	4	
HL 0634 5016	40			0	NT	3	
HL 0635 1002	438			0	NT	4	
HL 0635 2011	23			2	T	4	
HL 0635 3025	47			0	NT	4	
HL 0635 5023	62			2	T	4	
HL 0636 2015	47			0	NT	4	

HL 0636 4015	23			1.5	T	4	1.9E-07
HL 0636 5016	1			2.5	T	4	
HL 0637 3020	146			1.5	T	4	
HL 0637 3028	65			0	NT	4	
HL 0637 4022	47			0	NT	4	
HL 0637 4023	146			1.5	T	4	
HL 0637 4025	23	+	-	1.5	T	4	
HL 0638 5028	1			2	T	4	1.6E-05
HL 0638 7006	448			2	T	4	
HL 0639 2009	1			2	T	4	
HL 0639 2021	1			2.5	T	4	
HL 0639 4022	624			0	NT	4	
HL 0639 4025	20			0	NT	4	
HL 0639 5028	47			0	NT	4	
HL 0640 1010	47			0.5	NT	4	
HL 0640 1051	47			0	NT	3	
HL 0640 3004	47			0.5	NT	2	
HL 0640 3009	23	+	+	0.5	NT	4	2.0E-09
HL 0640 4012	146	+	+	0	NT	3	<1E-9
HL 0640 4016	94			0	NT	4	1.7E-08
HL 0640 5008	62			2.5	T	4	4.8E-06
HL 0641 2019	20			0	NT	2	
HL 0641 3006	701	+	+	0.5	NT	4	
HL 0641 3007	20			0	NT	4	
HL 0641 5012	177			2	T	4	
HL 0641 5021	9			0	NT	4	1.2E-08
HL 0641 5022	207			2	T	4	
HL 0642 1018	259			0	NT	4	
HL 0642 5019	444			0.5	NT	4	1.3E-08
HL 0642 5020	23			0	NT	4	
HL 0642 5021	75			2	T	4	
HL 0642 5022	47			0	NT	3	
HL 0643 3031	146	+	+	0	NT	4	4.0E-09
HL 0644 2011	1			3	T	3	
HL 0645 2023	62			3	T	4	
HL 0646 1021	65			0	NT	4	
HL 0646 2023	37			0	NT	4	
HL 0646 5011	23			2.5	T	4	
HL 0647 2033	181			0	NT	4	6.9E-09

HL 0647 5014	20	+	+	0	NT	3	3.4E-09
HL 0648 2012	59			2	T	3	
HL 0648 5020	9			0	NT	3	
HL 0648 5023	42			2	T	4	
HL 0650 4059	20			0	NT	4	
HL 0651 1014	23			3	T	4	
HL 0652 4035	96			1.5	T	4	
HL 0701 3035	23			3	T	4	
HL 0702 5017	1			2.5	T	4	
HL 0703 3038	23			2	T	4	
HL 0703 5020	23	+	-	2.5	T	4	
HL 0705 5011	47			0	NT	4	
HL 0707 2036	224			0	NT	4	6.2E-09
HL 0709 3014	18			3	T	4	4.1E-06
HL 0710 2013	75			2	T	4	
HL 0710 5012	47			0	NT	4	
LG 0712 2011	1			3	T	4	3.1E-05
LG 0713 5012	1			3	T	4	
LG 0714 2022	59			0	NT	3	
LG 0714 4016	20			0	NT	4	
LG 0715 5014	23			2	T	4	
LG 0716 2016	1			3	T	4	
LG 0717 5021	40			1	T	4	
LG 0721 1006	702			1	T	4	1.8E-06
LG 0721 5005	23			2	T	4	
LG 0723 4019	23	+	+	0	NT	3	
LG 0723 4026	23	+	+	0.5	NT	4	
LG 0724 2038	23			2.5	T	4	4.5E-06
LG 0724 2039	82	+	+	0	NT	3	
LG 0724 3029	703	+	+	1	T	4	
LG 0724 5003	6			2	T	4	1.5E-06
LG 0724 5013	708			0	NT	4	<1E-9
LG 0725 2030	1			2	T	4	
LG 0725 4014	1			3	T	4	
LG 0725 5007	94			0	NT	4	2.7E-08
LG 0726 2016	146			1	T	3	
LG 0726 4009	94			0	NT	3	
LG 0727 3031	96			0.5	NT	4	
LG 0727 4020	37			1	T	4	

LG 0727 5009	146			1.5	T	4	
LG 0727 5020	23			2	T	4	7.8E-07
LG 0727 5021	77			0	NT	3	
LG 0728 1015	44			1.5	T	4	
LG 0728 3011	23	+	+	0	NT	1	
LG 0729 4019	704			2	T	4	
LG 0751 3022	47			0	NT	3	
OLDA	ND			2	T	4	
130B	ND			1.5	T	4	
Lens	15	+	+	0	NT	4	<1E-9

Table S2. RNAseq analysis of the 3009ΔpLPL and 3009ΔrocRp strains relative to the wild-type 3009 isolate (HL 0640 3009).

Total RNA from three independent bacterial cultures grown to an OD 600 of 1.8-2.0 at 30°C was extracted, purified, and sequenced (Illumina). The number of reads was normalized, and the statistical significance (P_{adj}) of the fold change (FC) was determined with DEseq2. List is limited to chromosomal genes for which log_2FC is >1 in either of the two comparisons.

gene names	Gene identifier in isolate 3009	Gene identifier in the Paris strain	log2FC ΔpLPL vs WT	log2FC ΔrocRp vs WT	P_{adj} ΔpLPL vs WT	P_{adj} ΔrocRp vs WT
comM	STR10_v2_170063	lpp0640	3.32	2.00	3.69E-99	4.66E-34
comEA	STR10_v2_50169	lpp0872	3.84	2.47	2.40E-80	8.76E-32
comEC	STR10_v2_170020	lpp0680	2.72	1.75	4.28E-44	3.97E-17
	STR10_v2_270143	lpp2554	2.93	2.17	5.23E-41	6.50E-21
radC	STR10_v2_270142	lpp2553	2.01	1.32	4.00E-26	3.32E-10
	STR10_v2_110039	lpp1977	1.65	1.32	1.53E-13	1.67E-07
comF	STR10_v2_160037	lpp2280	1.47	1.02	1.31E-09	1.52E-03
	STR10_v2_110037	lpp1976	1.08	0.49	3.26E-06	2.44E-01
pilE	STR10_v2_50147	lpp0851	1.23	0.95	8.86E-06	1.68E-02

Table S3. Bacterial strains used or generated in this study.

A comprehensive list of *L. pneumophil*a clinical isolates used in this study are listed in Table S1. Abbreviations of antibioresistance are as follows: Gent for Gentamycin, Kan for Kanamycin and Strep for Streptomycin.

Strains	**Genotype and/or description**	**Reference**
Paris WT	Paris outbreak isolate CIP107629	CNR Lyon
Paris_S	Spontaneous streptomycin-resistant mutant of Paris; $Strep^R$	This study
Paris H1	*lpp0858a*::(J23119-sfGFP-*aacC*1); $Gent^R$	This study
HL-0640-3009	Clinical isolate "3009"	CNR Lyon
3009 $pLPL^{3009KF}$	pLPL::(*lacI*q, Ptac-*mazF*, *npt*II); Kan^R, $IPTG^S$	This study
3009ΔpLPL	3009 $pLPL^{3009KF}$ that lost pLPL; Kan^S, $IPTG^R$	This study
3009 ΔrocRp::kan-mazF	HL_0640_3009; ΔrocRp::(*lacI*q, Ptac-*mazF*, *npt*II); Kan^R, $IPTG^S$	This study
3009Δ*rocRp*	HL_0640_3009; ΔrocRp; Kan^S, $IPTG^R$	This study
Paris_S $pLPL^{3009KF}$	Transconjugant of 3009 $pLPL^{3009KF}$ and Paris_S; $Strep^R$, Kan^R, $IPTG^S$	This study
Paris $rocC_{TAA}$	Paris; $rocC_{TAA}$ (=$lpp0148_{TAA}$); *rocC* allele with a premature stop codon TAA	(6)
Paris Δ*rocR*	Paris; Δ*rocR*	(7)
Paris pLPP::*rocRp*	Paris; pLPP::*(rocRp-aacC*1); $Gent^R$	This study
$rocC_{TAA}$ pLPP::*rocRp*	$rocC_{TAA}$ pLPP::*(rocRp-aacC*1); $Gent^R$	This study
Δ*rocR* pLPP::*rocRp*	Δ*rocR* pLPP::*(rocRp-aacC*1); $Gent^R$	This study
LG-0712-2011_S	Spontaneous streptomycin-resistant mutant of LG-0712-2011; $Strep^R$	This study
HL-0638-5028_S	Spontaneous streptomycin-resistant mutant of HL-0638-5028; $Strep^R$	This study
LG-0712-2011_S $pLPL^{3009KF}$	Transconjugant of 3009 $pLPL^{3009KF}$ and LG-0712-2011_S; $Strep^R$, Kan^R, $IPTG^S$	This study
HL-0638-5028_S $pLPL^{3009KF}$	Transconjugant of 3009 $pLPL^{3009KF}$ and HL-0638-5028_S; $Strep^R$, Kan^R, $IPTG^S$	This study
HL-0438-2026	Environmental isolate of *Legionella geestiana*	CNR Lyon
HL-0427-4011	Environmental isolate of *Legionella israelensis*	CNR Lyon
Vestfold L18-01051	Environmental isolate of *Legionella israelensis*	Louise Kindingstad
JR32	Philadelphia-1 derivative; $Strep^R$; r − m +	(14)

Table S4. Oligonucleotides used in this study.

Oligonucleotide name	Sequence (5' to 3')	Used for
MazFk7-F	CGACTCACTATAGGGCGAATTGGGCCGCTTTCCAGTCGGGAAACCTG	PCR amplication of kan-mazF cassette
MazFk7-R	CATATGCCACCGACCCGAGCAAACCCGAAGAAGTTGTCCATATTGGCCAC	PCR amplication of kan-mazF cassette
DeltaRocRlike_P1	CTGCAGCTGAATAAGCTGGGTTATCC	Inserting the kan-mazF cassette in rocRp gene
DeltaRocRlike_P2	GGCCCAATTCGCCCTATAGTGAGTCGGTCCAACCTCGCTTGTTAAGCAAG	Inserting the kan-mazF cassette in rocRp gene
DeltaRocRlike_P3	GGGTTTGCTCGGGTCGGTGGCATATGCCAGCCCTTTCTACTTTGAATAATCTAC	Inserting the kan-mazF cassette in rocRp gene
DeltaRocRlike_P4	ATCATAATGAGGTGCTCACAAACAGTG	Inserting the kan-mazF cassette in rocRp gene
DeltaRocRlike_P2d	GTCCAACCTCGCTTGTTAAGCAAG	Deleting rocRp by removing the previously inserted kan-mazF cassette
DeltaRocRlike_P3d	CTTGCTTAACAAGCGAGGTTGGACCCAGCCCTTTCTACTTTGAATAATCTAC	Deleting rocRp by removing the previously inserted kan-mazF cassette
gnt-F	TTGCCCATGGACGCACACCGTG	PCR amplication of gentamicin cassette
gnt-R	CTCCCCGCGCGTTGGCCGATTCATTAAGTGCCACCTGGCGGCGTTG	PCR amplication of gentamicin cassette
KP1	CTGACCCGGGTGAGCCTTACAATAAAGTTGG	PCR amplification of rocRp
KP2	AATAGCGGCCGCAGCGAATAGGAGGATAGATG	PCR amplification of rocRp
plpp0110_P1	GCCAAACGCTATCAGGAGTTACCTC	Inserting rocRp-gentR in gene plpp0110 of pLPP
plpp0110_P2g	GTTTCCACGGTGTGCGTCCATGGGCAAGATTGTCCCATCTCCTTGAACC	Inserting rocRp-gentR in gene plpp0110 of pLPP
plpp0110_P3g	TAATGAATCGGCCAACGCGCGGGGAGCGAAGAATCAAGAATAACGCCAC	Inserting rocRp-gentR in gene plpp0110 of pLPP
plpp0110_P4	CTGATGAGGCGCTGCGAAGAG	Inserting rocRp-gentR in gene plpp0110 of pLPP
plpp0110_P2_rocRlike	CATCTATCCTCCTATTCGCTGCGGCCGCTATTGATTGTCCCATCTCCTTGAACC	Inserting rocRp-gentR in gene plpp0110 of pLPP
gnt-F_rocRlike	CCAACTTTATTGTAAGGCTCACCCGGGTCAGTTGCCCATGGACGCACACCGTG	Inserting rocRp-gentR in gene plpp0110 of pLPP
lpp0858_P1	ATCCTTCTCATTTAGAGAGGGATGCT	Inserting P23119-sfGFP in lpp0858

lpp0858_P2	TAAGTTGGACTTTCCCTTACTGGCTTCGGATGATTCCTGCAATGCT	Inserting P23119-sfGFP in lpp0858
J23119_F	GCCAGTAAGGGAAAGTCCAACTTATTGACAGCTAGCTCAGTCCTAGGTATAATTTCACACAGGAAACAGAATTC	Inserting P23119-sfGFP in lpp0858
term_R	GTTTCCACGGTGTGCGTCCATGGGCAAACGCAAAAAGGCCATCCGTC	Inserting P23119-sfGFP in lpp0858
gnt-F	TTGCCCATGGACGCACACCGTG	Inserting P23119-sfGFP in lpp0858
Cassette_Gm_Rv	TTCCCCGAAAAGTGCCACCT	Inserting P23119-sfGFP in lpp0858
lpp0858_P7	AGGTGGCACTTTTCGGGGAAGTACAACGACGAGAGACCGCA	Inserting P23119-sfGFP in lpp0858
lpp0858_P9	TGTGCAGACATACCCTCCCATA	Inserting P23119-sfGFP in lpp0858
rpsL_Fw	GCAGCTCCAGATGGCTCAATC	PCR amplication of rpsL region (4kb)
rpsL_Rv	CAACCATACATGTCCATATTGACCAC	PCR amplication of rpsL region (4kb)
mazF-pLPL_P1F	GGTATTCAGTTGATCAATTCCCTTCG	Inserting kan-mazF cassette in a pseudogene of pLPL^{3009}
mazF-pLPL_P2F	GGCCCAATTCGCCCTATAGTGAGTCGACATCTGAGACTGATGAGTAACC	Inserting kan-mazF cassette in a pseudogene of pLPL^{3009}
mazF-pLPL_P3F	GGGTTTGCTCGGGTCGGTGGCATATGCTGATCATCGATGGAACAGACAATTTTG	Inserting kan-mazF cassette in a pseudogene of pLPL^{3009}
mazF-pLPL_P4F	GATGGTAGATACTTTGCATCTGGC	Inserting kan-mazF cassette in a pseudogene of pLPL^{3009}
RT19-rocRlike	AGTGGGTCACAGCTTGATGAGAAAGGGCTGGTCGTGTG	RT-PCR RocC-bound RNA
RT20-rocR	AGTGGGTCACAGCTTGATGAGAAAGGGCCAATCAGTGTG	RT-PCR RocC-bound RNA
RRl17-F	GCGAGGTTGGACTTGCT	RT-PCR RocC-bound RNA
RRl20-R	AGTGGGTCACAGCTTGATG	RT-PCR RocC-bound RNA
LA124_RACE_RocR-R	TGACACATAGCAAGTCCAAC	RACE mapping
LA125_RACE_RocR-F	TTCCACTGGGTCAATTGGCG	RACE mapping
LA126_RACE_RocRlike-F	ATCCAATGGGTGTGGTCGCG	RACE mapping
comEA-NB2	Biotin-CTACAAAACGCTGCCCTATACCCTTGACTTCCGCAAGCTCTTCCAGAG-Biotin	Northern-blot probe for dectection of comEA
LA59_rocR-small-NB	Biotin-TGTGTCGCCAATTGACCCAGTGGAATGACACATAGCAAGTCCAACCTC-Biotin	Northern-blot probe for dectection of RocR
rocR-pLPL-NB2	Biotin-GCTGGTCGTGTGTCGCGACCACACCCATTGGATTGACACAA-Biotin	Northern-blot probe for dectection of RocRp

Table S5. Plasmids used in this study.

Plasmid name	Reference	Used for
pXDC18	(15)	Template for PCR of gentamicin resistance gene
pASG-1	(16)	Template for PCR of sfgfp gene
pGEM-kan-mazF (pGEM-MK)	(1)	Template for kan-mazF cassette
pGEM-ihfB::kan	(6)	Natural transformation assay. Plasmid carrying a kanamycin resistance gene in a 4kb *L. pneumophila* chromosomal region encompassing the *ihfB* gene
pX3-rocRp	(2)	Complementation plasmid, expressing RocRp from its native promoter

Figures S1 to S7

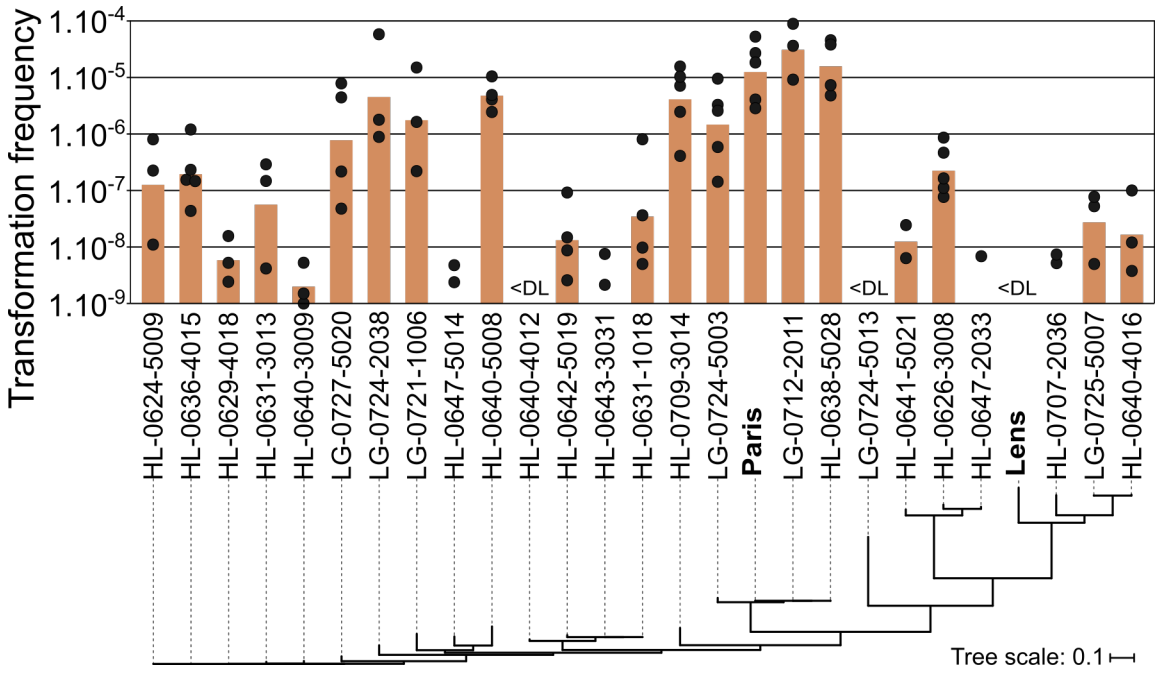

Figure S1. Extensive variations of the trait of natural transformation are inconsistent with the phylogeny.

Quantitative analysis of natural transformability of 25 isolates of *L. pneumophila*. Natural transformation was tested by incubating each isolate with a non-replicative plasmid carrying the *ihfB* gene interrupted by a gene conferring resistance to kanamycin. Each isolate was tested from three to five times on independent occasions. Bars represent the geometric mean when at least two frequencies (black dots) could be determined. <DL, below detection limit. A region homologous to the transforming DNA is present in all tested isolates. Phylogenetic relationships were computed based on core-genome SNPs and displayed as a phylogram.

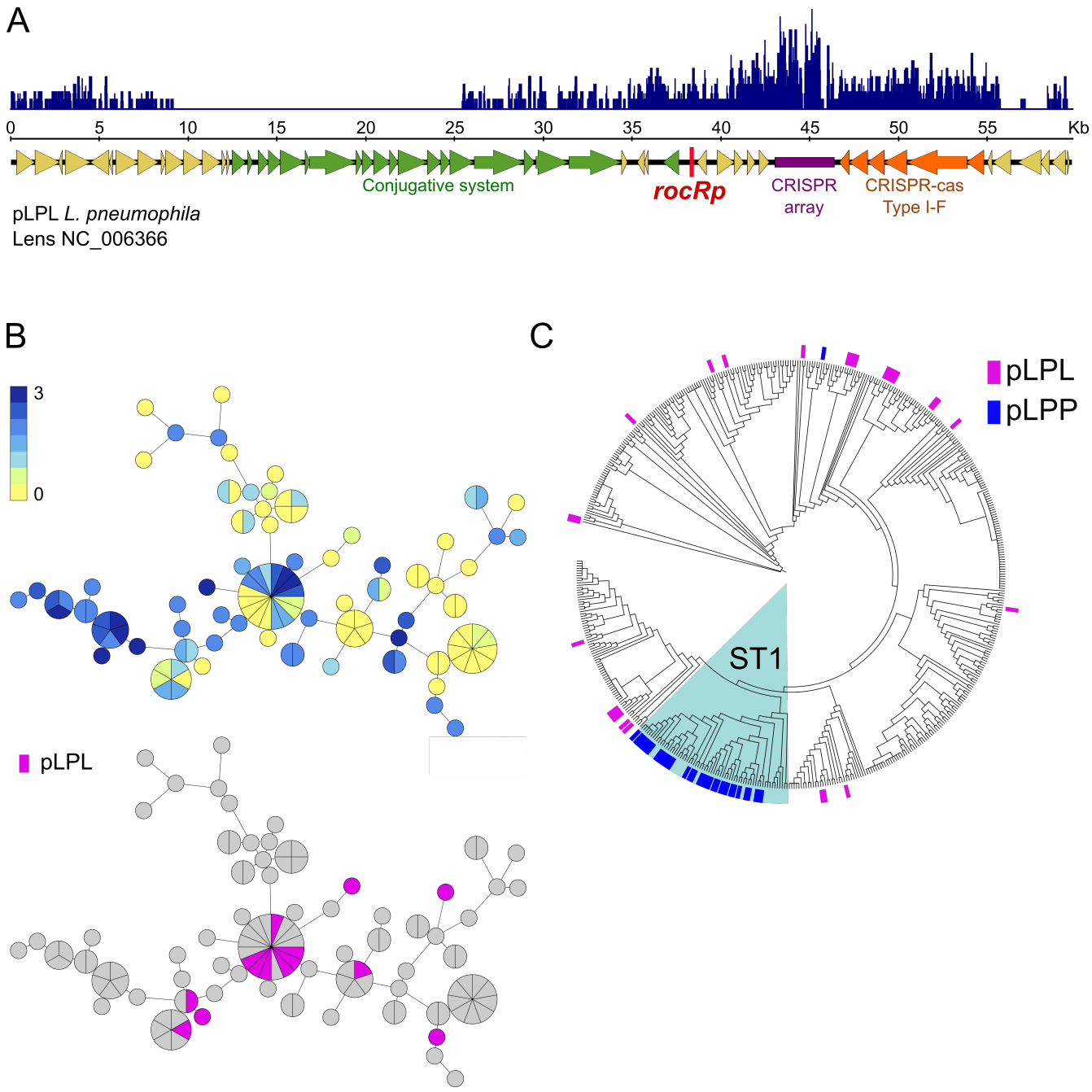

Figure S2. Plasmid pLPL associates with low levels of natural transformation.

A. Linear map of plasmid pLPL from the Lens isolate. Sequences of the 827 unambiguous sequences identified by DBGWAS as associating with the non-transformable phenotype (q<0.1) were mapped on the pLPL sequence (blue bars). B. Top: Semi-quantitative analysis of natural transformability of 113 isolates of *L. pneumophila*. Transformability was determined using a PCR product encompassing a *rpsL* allele conferring resistance to streptomycin. Genetic relationship were determined by cgMLST and visualized using a minimum spanning tree displaying transformation scores color coded from 0 (yellow) to 3 (dark blue). Bottom: Presence of the pLPL plasmid (pink) in the panel of 113 isolates tested for transformability. C. Cladogram based on core-genome SNPs of 537 *L. pneumophila* genomes with presence of pLPL (blue) and pLPL (pink).

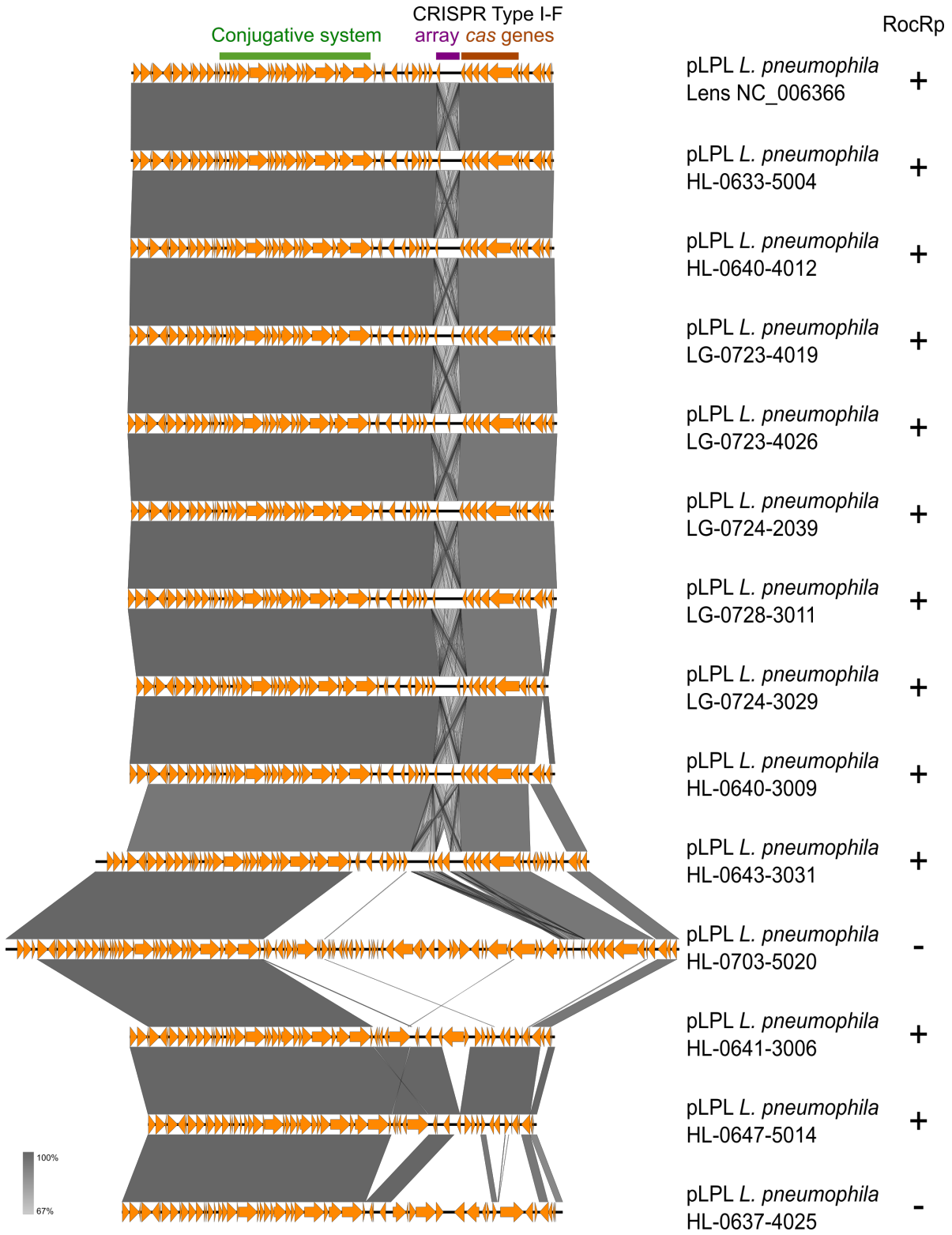

Figure S3. Multiple alignment of the 14 pLPL variants found in the panel of 113 clinical isolates investigated for their transformability levels.

Plasmids pLPL from HL-0703-5020 and HL-0637-4025 present large insertions/deletionsand the absence of *rocRp*, which is consistent with their transformable phenotype.

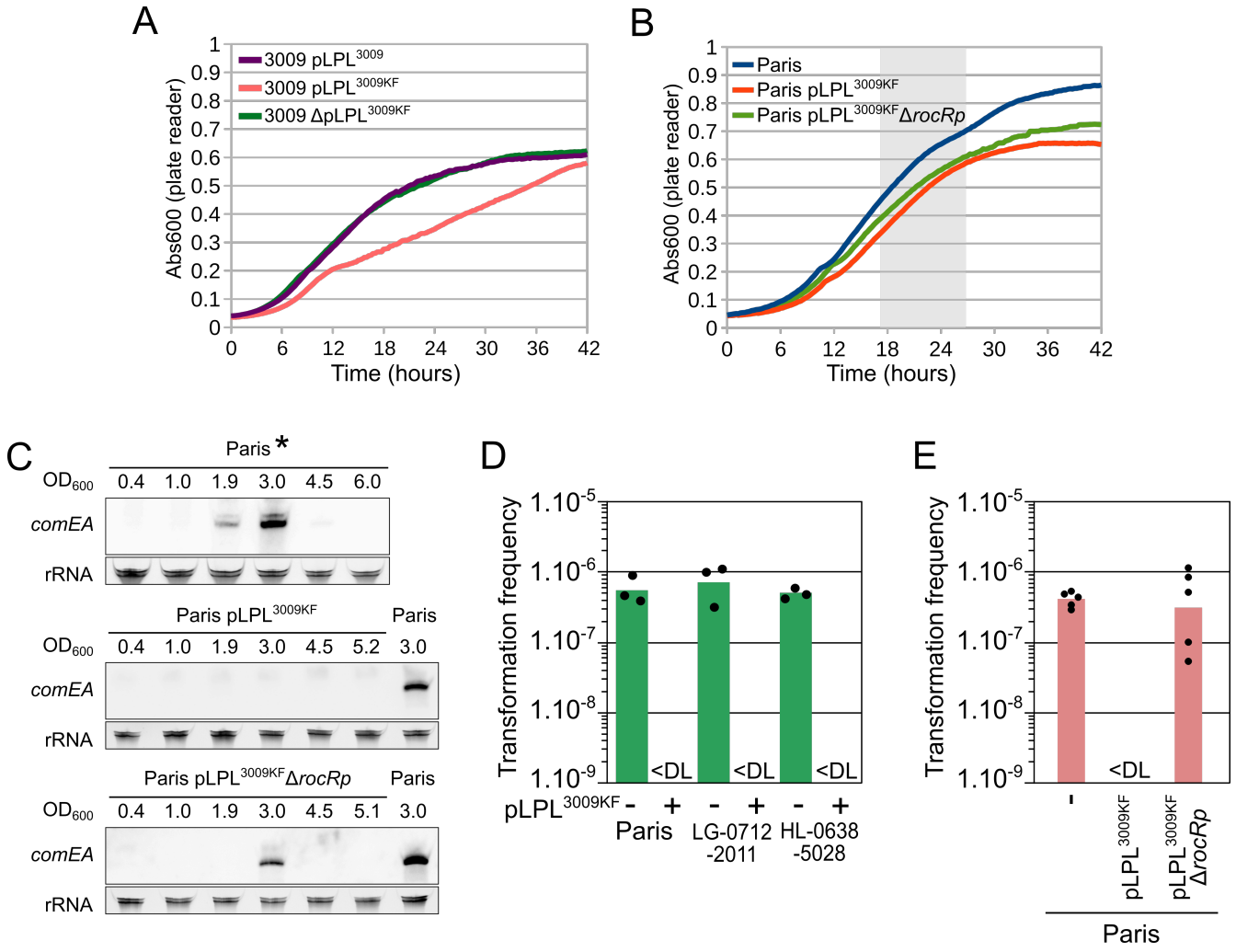

Figure S4. Conjugative transfer of pLPL inhibits natural transformation of its new bacterial hosts.

A. Growth curve at 30°C of the 3009 isolate, carrying or not the original pLPL^{3009} or the variant pLPL^{3009KF} in which the kan-mazF cassette was inserted. Growth was monitored in a microplate reader.

B. Growth curve at 30°C of the Paris strain and its transconjugants carrying the intact pLPL^{3009KF} or the pLPL^{3009KF} deleted of *rocRp*. Growth was monitored in a microplate reader. Growth in 3 mL liquid medium in tubes shows similar kinetic, with a lower OD in stationary phase for the strains carrying pLPL^{3009KF} or pLPL^{3009KF}Δ*rocRp* (~5) than for Paris (~6). C. Northern-blot analysis of *comEA* expression during growth of Paris (* data are reproduced from Fig. 3A) and its transconjugants carrying pLPL^{3009KF} or pLPL^{3009KF}Δ*rocRp*. In each northern-blot, a sample of the Paris strain expressing *comEA* (OD=3) is loaded to serve as a reference. D and E. Natural transformability of Paris and clinical isolates compared to their transconjugants carrying pLPL from isolate 3009 bearing the kan-mazF cassette or its derivative deleted of *rocRp*. Spontaneous streptomycin-resistant mutants of the tested strains were first isolated and used as recipients of conjugative transfer of pLPL^{3009KF} or pLPL^{3009KF}Δ*rocRp*. Natural transformation was tested with genomic DNA from a gentamycin-resistant strain (Paris_H1). <DL, below detection limit.

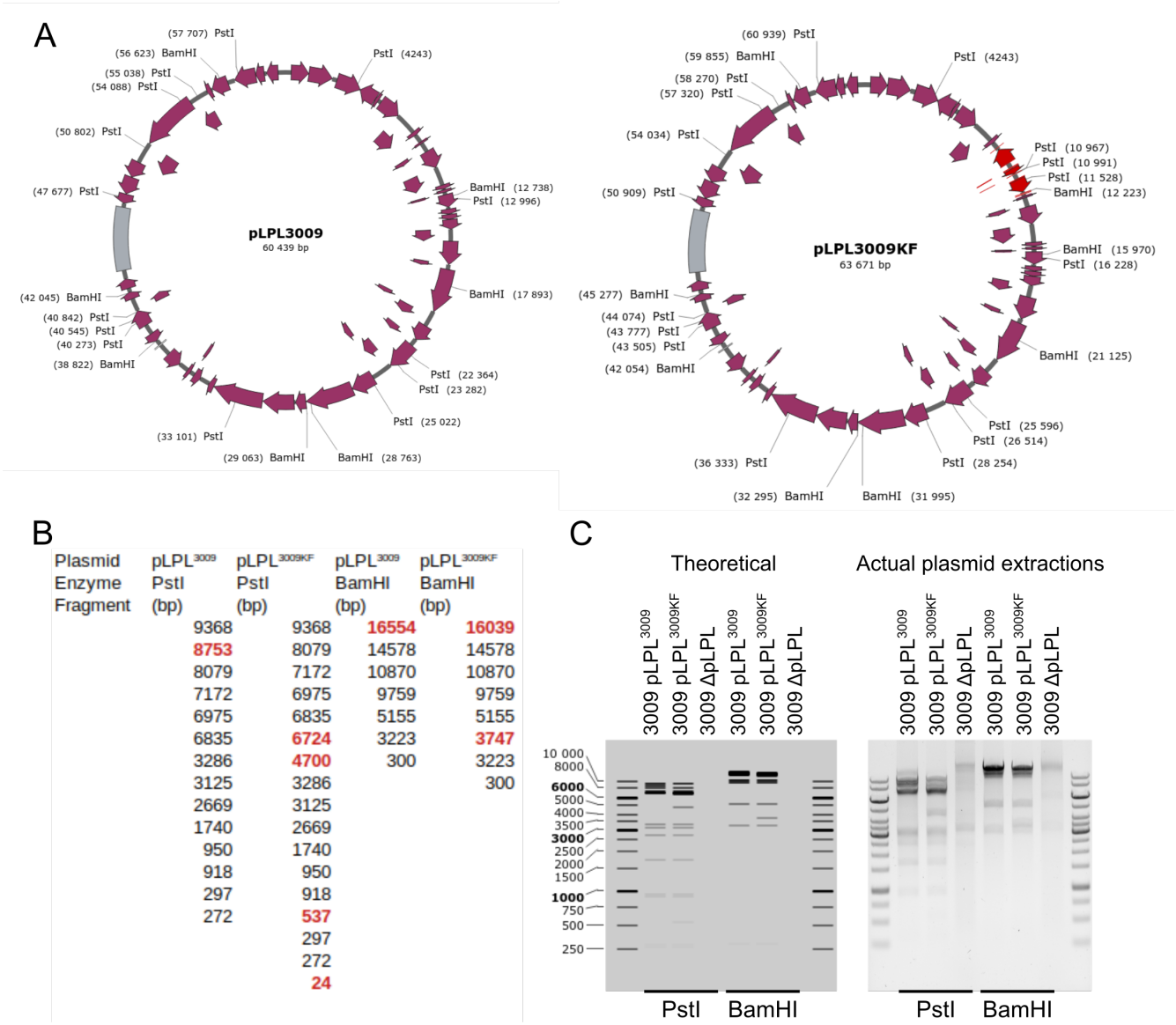

Plasmid	pLPL3009	pLPL3009KF	pLPL3009	pLPL3009KF
Enzyme	PstI	PstI	BamHI	BamHI
Fragment	(bp)	(bp)	(bp)	(bp)
	9368	9368	16554	16039
	8753	8079	14578	14578
	8079	7172	10870	10870
	7172	6975	9759	9759
	6975	6835	5155	5155
	6835	6724	3223	3747
	3286	4700	300	3223
	3125	3286		300
	2669	3125		
	1740	2669		
	950	1740		
	918	950		
	297	918		
	272	537		
		297		
		272		
		24		

Figure S5. Characterisation of isolate 3009 cured of pLPL.

A. Map of pLPL3009 and pLPL3009KF with restriction sites of PstI and BamHI. B. List of restriction fragments generated by PstI or BamHI digests of the two plasmids. C. Restriction profiles of plasmid extraction from the clinical isolate HL-0640-3009 and mutants. Specific fragments are shown in red. As expected, introduction of the kan-mazF cassette generates a different restriction profile due to the presence in the cassette of PstI and BamHI restriction sites. Plasmid pLPL is effectively absent from isolate 3009ΔpLPL. A smear is still visible due to the presence of contaminating genomic DNA in the plasmid preparation.

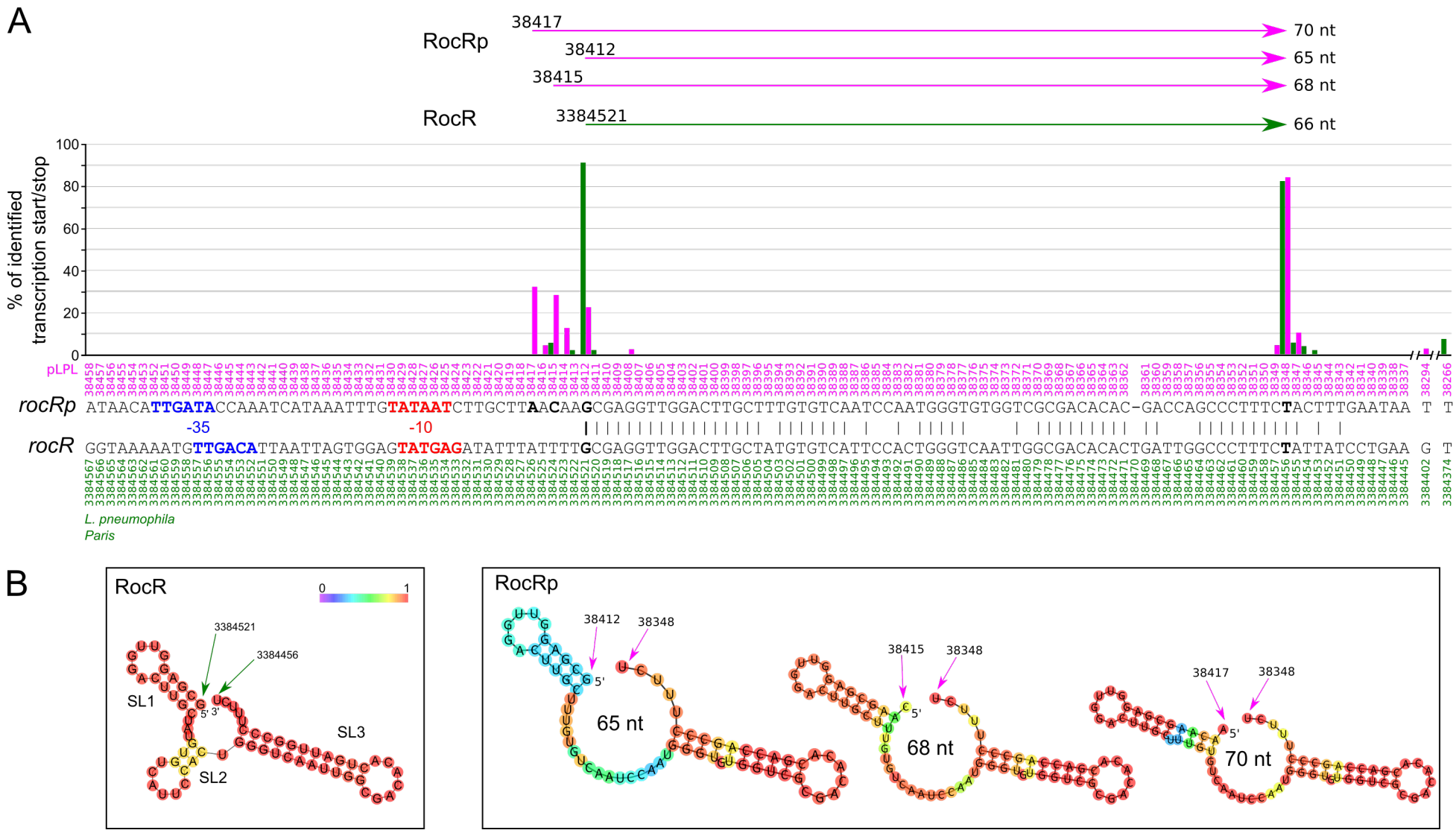

Figure S6. RACE determination of the 5' and 3' ends of RocR and RocRp.

A. Relative abundance of identified 5' and 3'end of RocR (green) and RocRp (magenta). The sequence of the pLPL and the chromosome of the Paris strains are aligned based on the homology of the *rocR* and *rocRp* genes. Sequences highlighted in blue and green represent putative -10 and -35 box of the promoter, respectively. Nucleotides in bold font correspond to the mapped transcription start and termination sites. B. Secondary structures predicted by RNAfold (17) of the RNA sequences identified for RocR and RocRp.

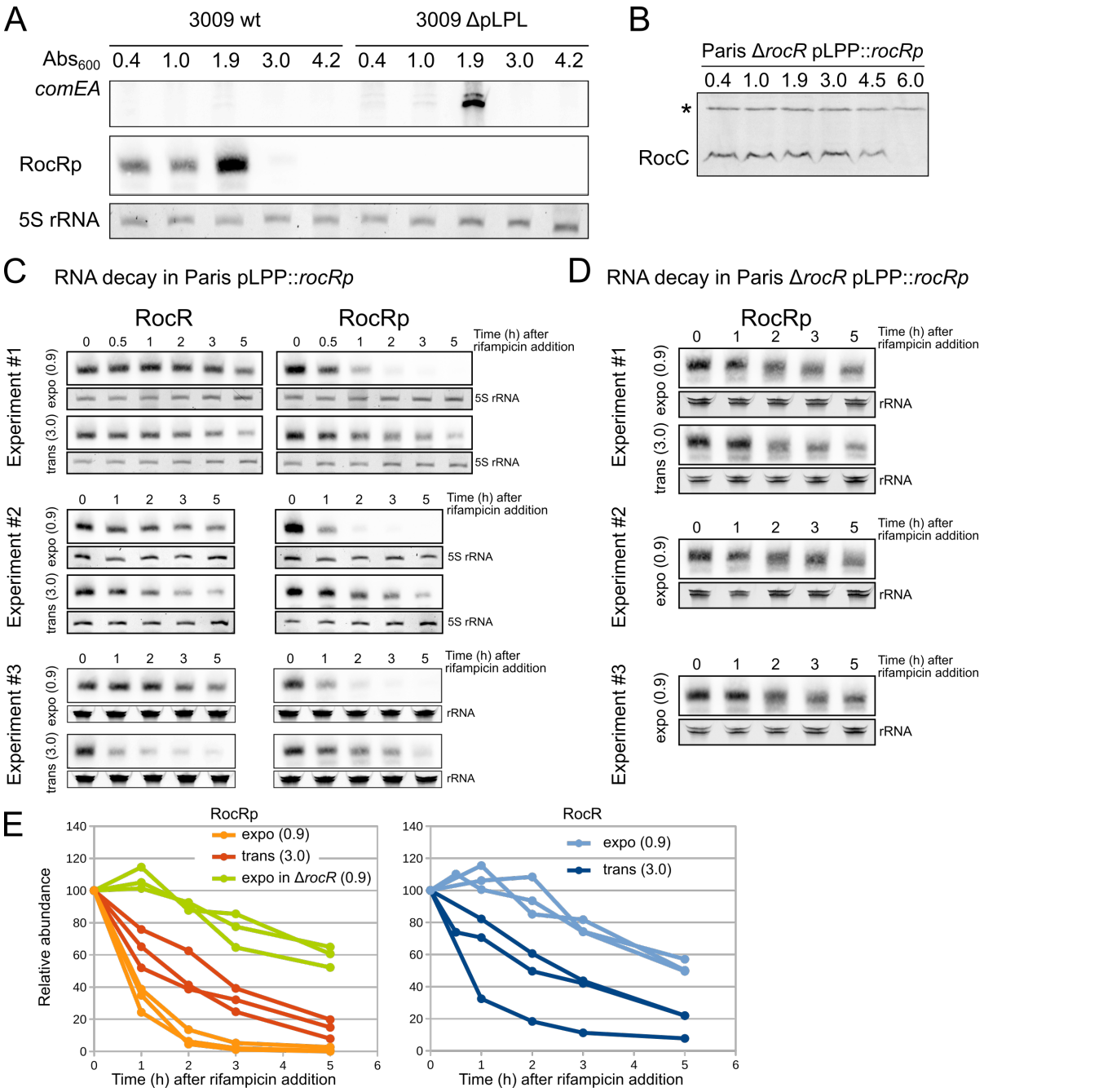

Figure S7. Northern-blot analyses.

A. Northern-blot analysis of *comEA* mRNA and RocRp expression during growth of strains 3009 and 3009ΔpLPL in AYE medium at 30°C. Total RNAs were extracted at the indicated optical densities (measured at 600 nm, OD_{600}) of the culture, and corresponding to the exponential growth phase (0.4 to 1.0), the transition phase (1.9) and early (3.0) and late stationary phase (4.2). Total RNAs were separated on an 8% denaturing polyacrylamide gel. RocR and *comEA* mRNAs were revealed with a biotinylated oligonucleotide probe. 5S rRNA was used as a loading control. B. Western-blot analysis of RocC expression during growth at 30°C of the Paris strain carrying the *rocRp* gene on pLPP (Paris pLPP::*rocRp*). Total soluble proteins were extracted at the indicated optical densities (OD_{600}) of the culture, during the exponential growth phase (0.4 to 1.0), the transition phase (1.9 and 3.0) and the early (4.5) and late stationary phase (6.0). The star (*) indicates a cross-reactive band. C. Northern-blot experiments used to determine the half-life of RocR and RocRp in exponential phase (0.9) and transition phase (3.0) in the strain Paris pLPP::*rocRp*. When the cultures reached the indicated optical densities (0.9 and 3.0), rifampicin was added at 100 µg/mL to block transcription and samples were removed at the indicated times after addition of rifampicin. Total RNA was extracted and expression of RocR and RocRp was analysed by northern-blot. Signal intensities were determined using densitometry, normalized to rRNA levels and were fit to a first-order exponential decay with the Qtiplot software. Each experiment shown (#1, #2 and #3) was conducted on separate occasions, several days or weeks apart. D. Same as in C but with the strain Paris pLPP::*rocRp* deleted of the *rocR* gene. E. Graphed quantification of northern-blot of C and D. RocR and RocRp levels were determined by densitometry, normalized to rRNA levels and levels at time 0 were set to 100.

SI References

1. Bailo N, et al. (2019) Scar-Free Genome Editing in Legionella pneumophila. *Methods Mol Biol Clifton NJ* 1921:93–105.
2. Charpentier X, Kay E, Schneider D, Shuman HA (2011) Antibiotics and UV Radiation Induce Competence for Natural Transformation in Legionella pneumophila. *J Bacteriol* 193(5):1114–1121.
3. Silva M, et al. (2018) chewBBACA: A complete suite for gene-by-gene schema creation and strain identification. *Microb Genomics*. doi:10.1099/mgen.0.000166.
4. Zhou Z, et al. (2018) GrapeTree: visualization of core genomic relationships among 100,000 bacterial pathogens. *Genome Res* 28(9):1395–1404.
5. Jaillard M, et al. (2018) A fast and agnostic method for bacterial genome-wide association studies: Bridging the gap between k-mers and genetic events. *PLOS Genet* 14(11):e1007758.
6. Juan P-A, Attaiech L, Charpentier X (2015) Natural transformation occurs independently of the essential actin-like MreB cytoskeleton in Legionella pneumophila. *Sci Rep* 5:16033.
7. Attaiech L, et al. (2016) Silencing of natural transformation by an RNA chaperone and a multitarget small RNA. *Proc Natl Acad Sci U S A* 113(31):8813–8818.
8. Soutourina OA, et al. (2013) Genome-wide identification of regulatory RNAs in the human pathogen Clostridium difficile. *PLoS Genet* 9(5):e1003493.
9. Bolger AM, Lohse M, Usadel B (2014) Trimmomatic: a flexible trimmer for Illumina sequence data. *Bioinforma Oxf Engl* 30(15):2114–2120.
10. Wick RR, Judd LM, Gorrie CL, Holt KE (2017) Unicycler: Resolving bacterial genome assemblies from short and long sequencing reads. *PLoS Comput Biol* 13(6):e1005595.
11. Seemann T (2014) Prokka: rapid prokaryotic genome annotation. *Bioinforma Oxf Engl* 30(14):2068–2069.
12. Abby SS, Néron B, Ménager H, Touchon M, Rocha EPC (2014) MacSyFinder: a program to mine genomes for molecular systems with an application to CRISPR-Cas systems. *PloS One* 9(10):e110726.
13. Cury J, Touchon M, Rocha EPC (2017) Integrative and conjugative elements and their hosts: composition, distribution and organization. *Nucleic Acids Res* 45(15):8943–8956.
14. Sadosky AB, Wiater LA, Shuman HA (1993) Identification of Legionella pneumophila genes required for growth within and killing of human macrophages. *Infect Immun* 61(12):5361–73.
15. Charpentier X, Faucher SP, Kalachikov S, Shuman HA (2008) Loss of RNase R Induces Competence Development in Legionella pneumophila. *J Bacteriol* 190(24):8126–36.
16. Godeux A-S, et al. (2018) Fluorescence-Based Detection of Natural Transformation in Drug-Resistant Acinetobacter baumannii. *J Bacteriol* 200(19):e00181-18.
17. Lorenz R, et al. (2011) ViennaRNA Package 2.0. *Algorithms Mol Biol AMB* 6:26.